

# HiSST: 4th International Conference on High-Speed Vehicle Science Technology 22 -26 September 2025, Tours, France



# Application of Machine Learning to the Evaluation of the Flight Conditions in the Hypersonic Flight Experiment

Susumu Hasegawa 1

#### **Abstract**

The Japan Aerospace Exploration Agency (JAXA) conducted a hypersonic combustion flight test to resolve the wind tunnel dependency. The test vehicle was launched by the S-520 small rocket into a ballistic flight orbit, and the combustion experiment was conducted when it reached Mach number during the descent. The JAXA RD1 flight test vehicle was launched by the S-520 rocket from JAXA Uchinoura Space. On July 24, 2022, the flight test was successfully conducted and flight experiment data was collected. Based on the ADS data evaluated by CFD, this study attempted to improve the prediction of dynamic pressure using linear weight analysis and statistical machine learning algorithms. As a result, it was found that the results were more promising than the dynamic pressure estimation formulation initially used. In particular, xgboost provides the closest estimate to the theoretical values.

Keywords: Hypersonic, Flight Test, Scramjet, Machine Learning

## **Nomenclature**

ADS - Air Data Sensor

CFD - Computational Fluid Dynamics

Cp - Pressure coefficient

GBDT - Gradient-Boosting Decision Tree

IMU - Inertial Measurement Unit

M - Mach number

MAE - Mean Absolute Error
Q - Dynamic pressure, kPa
R2 - Coefficient of Determination
RMSE - Root Mean Squared Error

x, y, z - Axis coordinates a - Angle of attack, ° β - Angle of sideslip, °

subscript

#### 1. Introduction

Research on hypersonic flight propulsion is a fundamental technology indispensable for the realization of next-generation aerospace transportation systems, and in recent years, rapid progress has been

Page | 1
Paper Title : Application of Machine Learning to the Evaluation of the Flight Conditions in the Hypersonic Flight Experiment
Copyright © 2025 by author(s)

<sup>&</sup>lt;sup>1</sup> Japan Aerospace Exploration Agency, Kakuda, Miyagi, 981-1525, Japan, <a href="mailto:haseqawa.susumu@jaxa.jp">haseqawa.susumu@jaxa.jp</a>

made worldwide. In particular, propulsion systems in the flight regime above Mach number 5 are difficult to handle with conventional turbo engines and ramjets, and there is a strong need to establish a new engine concept. Against this background, the scramjet (supersonic combustion ramjet, scramjet) engine is widely recognized as a promising candidate for hypersonic propulsion because of its structural simplicity and high Mach number adaptability utilizing supersonic combustion [1-9].

Scramjet research has been vigorously pursued in the U.S. X-43A and X-51A, Australia's HyShot program, Europe, Russia, India, and China. These efforts have formed an international trend to verify the feasibility of propulsion systems through wind tunnel tests and computational fluid dynamics (CFD) analysis as well as demonstration tests in actual flight environments. However, the feasibility of hypersonic combustion has not been fully established, as it involves many technical issues such as fuelair mixing, flame retention, and combustion efficiency at short dwell times.

In the midst of these international research trends, the Japan Aerospace Exploration Agency (JAXA) conducted a hypersonic combustion flight experiment to overcome the limitations inherent in wind tunnel testing. The purpose of this experiment was to burn ethylene fuel under flight conditions of about Mach 6 to obtain combustion data in a real flight environment [10-12]. The test vehicle was injected into ballistic orbit by the S-520 small rocket, and a burn test was conducted during the descent process. To reduce attitude instability during descent, a flare was installed at the rear of the fuselage, and a design was adopted to ensure resilience and flight stability by utilizing drag forces.

In particular, the JAXA RD1 flight test vehicle was launched from the Uchinoura Space Center on July 24, 2022, and achieved its planned results in a flight experiment in July 2022. The flight data obtained are extremely valuable for demonstrating the feasibility of hypersonic combustion and will provide fundamental knowledge for future scramjet propulsion system design. In this paper, a method for estimating the flight state from the ADS (Air Data Sensor) system is studied based on the data from this flight experiment.

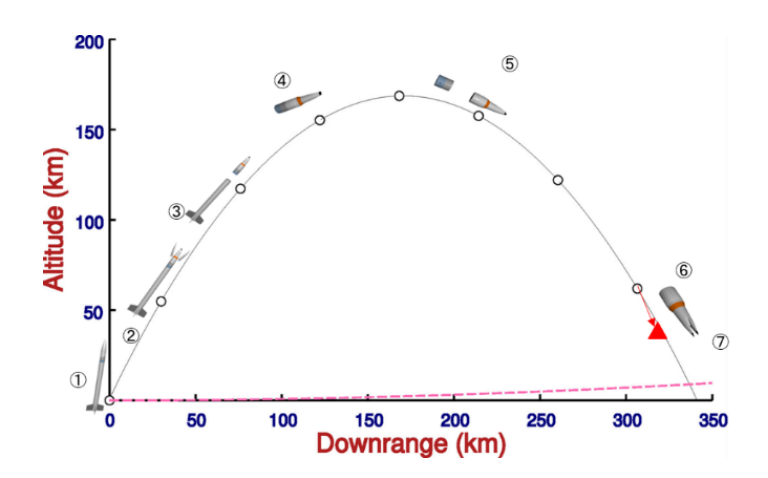


**Fig 1.** Schematic diagram of the hypersonic flight experiment.

## 2. Flight vehicle model

The flight vehicle model used in this study is shown in Fig. 2. The flight vehicle was comprehensively studied and designed from aerodynamic, thermal, and structural perspectives for application to a hypersonic combustion experiment. It consists of an inlet section, isolator section, combustor section, duct section, and rear flare. The flight test was designed for a Mach number of 6 and a dynamic pressure of about 50 kPa.

The geometric contraction ratio of the inlet section is set to 5, and the shock wave formed is designed to reach the shoulder of the duct inlet. According to two-dimensional shock wave theory, the oblique shock wave at the inlet increases pressure while the expansion wave generated behind it decreases pressure. While these effects cancel each other out, the overall design provides the pressure increase necessary for combustion to take place. In other words, the geometry of the inlet and isolator sections

is designed to meet the pressure conditions necessary to achieve hypersonic combustion.

In addition, a flare was installed at the rear of the fuselage to provide aerodynamic stabilization against disturbances that may occur during flight. The flares generate a restoring moment by increasing the drag force, which reduces the pitching and yawing instability behaviour expected during descent. The schematic structure of the aircraft and the attitude angles (pitch angle  $\alpha$  and yaw angle  $\beta$ ) are shown in Fig. 2. Fig.3 also shows the flight vehicle and the arrangement of the static pressure sensors used for the measurements. The red circles in the figure indicate the locations of the static pressure holes. These sensors measure the pressure distribution during the flight test and provide basic data that contributes to the identification of aerodynamic characteristics.

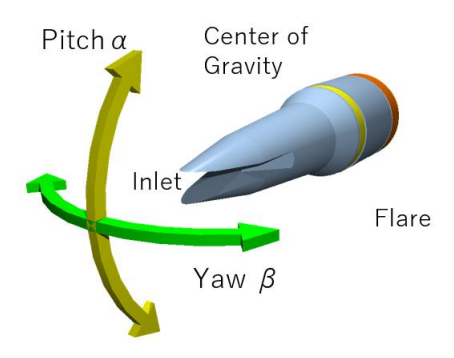


**Fig 2.** Schematic of the flight test vehicle and the pitch ( $\alpha$ ) and yaw ( $\beta$ ) directions.

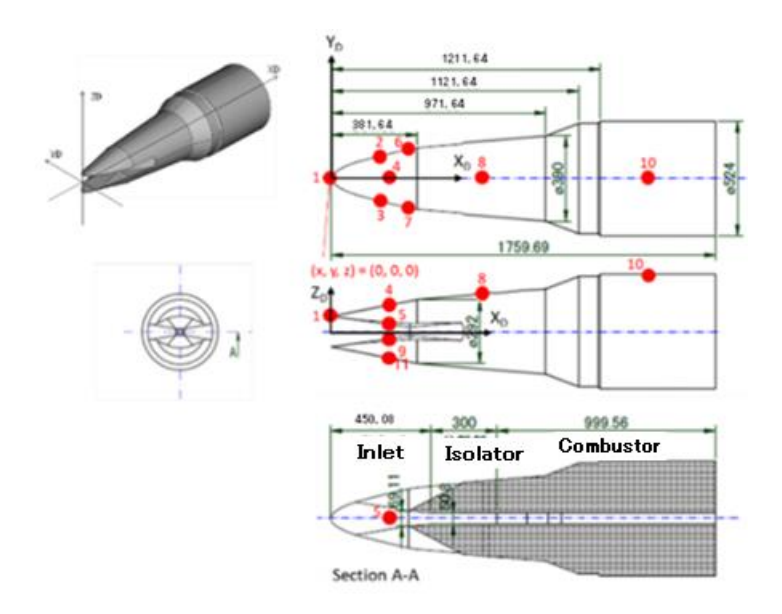


**Fig 3.** Configuration and dimensions of the flight test vehicle model, with the ADS installation locations indicated in red.

## 3. Numerical Computation around the Flight Vehicle Model

In order to plan and successfully conduct this flight experiment, various numerical analyses were conducted in advance. Specifically, these included aerodynamic and heat transfer analyses of the airframe surroundings, as well as high-precision simulations of the combustion behavior. These analyses were performed using the large-scale computational resources of the JSS3 supercomputer at the Japan Aerospace Exploration Agency (JAXA) Supercomputer Center. This paper focuses on these analyses, especially on the aerodynamic analysis around a hypersonic flight vehicle [13-25].

The unstructured mesh-based flow solver FaSTAR [13] was used for the aerodynamic analysis; FaSTAR is based on the cell-centered finite volume method and is capable of solving the compressible full

HiSST-2025-40
Page | 3 Paper

Navier-Stokes equations on an unstructured mesh, which has been validated in several benchmark test cases and has been validated in several benchmark test cases [14-17]. In this study, the HLLEW (Harten-Lax-van Leer-Einfeldt-Wada) method [18] is employed to evaluate the numerical fluxes, and the time integration is performed using LU-SGS (Lower/Upper Symmetric Gauss-Seidel) implicit method [19] was used for time integration. This method enables stable and efficient solution of strong shock waves and boundary layer interferences characteristic of hypersonic flows. To improve spatial accuracy, a second-order accuracy reconstruction was applied. Specifically, the Green-Gauss weighted least square (GLSQ) method [20] was used for gradient calculations, and Hishida's limiter [21] was introduced to further suppress numerical oscillations. For the turbulence model, the "SA-noft2-R" variant with Crot = 1 was employed, following the notation described in the NASA Langley Turbulence Model Resource (TMR) [22]. In this study, the analysis is based solely on this variant.

As representative results of the analysis, the pressure coefficient distribution acting on the surface of the flight vehicle and the Mach number distribution around the flight vehicle are shown in Fig. 4. The calculation conditions are based on a flight condition of Mach number 6 and angle of attack of 5°. These results provide important basic data for the interpretation of pressure measurements and burning behavior in flight experiments.

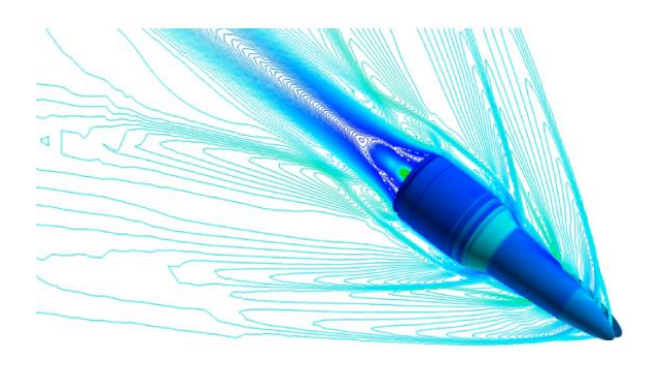


**Fig 4.** Pressure coefficient on the surface of the flight vehicle model and Mach number distribution around the model.

#### 4. Air Data Sensing System

Pitot tubes are usually used in flight condition measurements to estimate dynamic pressure and Mach number. However, as the aircraft approaches the hypersonic region, strong aerodynamic heating on the fuselage surface inevitably occurs, which is likely to damage the pitot tube structure and reduce measurement accuracy. It has also been pointed out that pitot tubes installed externally as projections cause increased aerodynamic drag and have a negative impact on overall flight performance. As a method to avoid such restrictions, a method of attaching pressure sensors directly to the outer surface of the aircraft and estimating the flight state from the obtained surface pressure distribution has been attracting attention. In particular, the use of Air Data Sensors (ADS) is a powerful method to estimate flight state quantities (angle of attack, yaw angle, dynamic pressure, Mach number, etc.) in real time and with high accuracy.

In this study, multiple ADSs were installed on the surface of the test vehicle, and the measurements obtained through flight experiments were analyzed. An example is shown in Figure 5. According to the analysis results, the pitch and yaw angles were generally within  $\pm 2^{\circ}$ , but the local surface pressure fluctuations were very large, confirming that the flow field was highly unsteady in time and space.

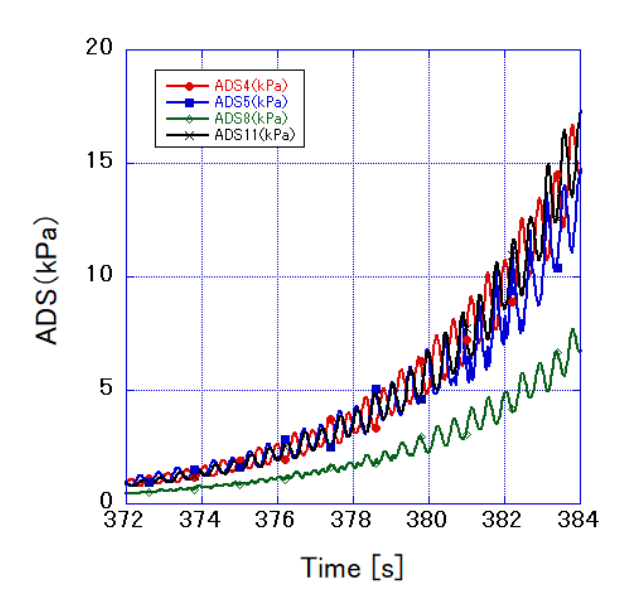


Fig 5. Time history of representative air data sensors during flight

## 5. Applications of Statistical Machine Learning

For the application of machine learning to the estimation of flight conditions from air data sensors (ADS), a three-step procedure is required. First, a training dataset must be constructed.

Step 1: Generation of training data by CFD

Computational fluid dynamics (CFD) simulations were carried out under the following conditions:

Mach numbers: 5.4, 5.5, 5.6, 5.7, 5.8, 5.9

Dynamic pressures: 10, 20, 30, 40, 50, 60, 70, 80, 90, 100 kPa

Angles of attack (a): -3, -2, -1, 0, 1, 2, 3°

Angles of sideslip ( $\beta$ ): -3, -2, -1, 0, 1, 2,  $3^{\circ}$ 

All combinations of  $\alpha$  and  $\beta$  were considered, and the corresponding ADS pressure values were obtained. These results were used to build the machine learning training dataset.

Step 2: Construction of machine learning models

Based on the CFD-derived training data, machine learning models were developed to establish the relationship between ADS pressure measurements and flight conditions.

Step 3: Application to flight test data

Finally, the pressure values measured by ADS during the flight experiment were used as input to the trained machine learning models, enabling the estimation of flight states such as dynamic pressure.

In our previous study, dynamic pressure evaluation formulas were analyzed using conventional multiple linear regression. In this section, we extend the analysis by employing statistical machine learning techniques to evaluate dynamic pressure [26-28]. Specifically, we introduce nonlinear regression approaches through the use of gradient boosting, which represents one of the most powerful machine learning methods.

Gradient boosting can be applied to both regression and classification tasks. It constructs predictive models as an ensemble of weak learners, typically decision trees. When decision trees serve as the weak learners, the resulting algorithm is referred to as gradient boosting decision trees (GBDT). GBDT effectively combines gradient descent optimization, boosting strategies, and decision tree models. Due to its high predictive accuracy and practical applicability, GBDT has been widely adopted in data analysis competitions, often outperforming random forests.

HiSST-2025-40 Page | 5 Paper Title : Application of Machine Learning to the Evaluation of the Flight Conditions in the Hypersonic Flight Experiment

Several representative GBDT libraries are commonly used in practice. *XGBoost* (eXtreme Gradient Boosting)[27], released in 2014, rapidly gained popularity owing to its robustness and computational efficiency, and has since been frequently employed in predictive modeling competitions. *LightGBM*, introduced in 2016, focuses on leaf-wise tree growth strategies to improve training efficiency for large-scale data. *CatBoost* [28], released in 2017, incorporates unique innovations such as effective handling of categorical features, making it particularly suitable for real-world data sets.

In the present study, we applied GBDT, CatBoost, and XGBoost to the problem of dynamic pressure evaluation. By comparing their performance against conventional linear multiple regression, we highlight the differences between traditional statistical approaches and modern machine learning methods. As shown in Table 1, the evaluation errors under different methodologies are systematically compared. Figure 6 illustrates the variation of RMSE and MAE for each algorithm. The results demonstrate that machine learning approaches achieve notable error reduction, with XGBoost providing the most significant improvement in this study.

Figure 6 shows a comparison of the theoretical and estimated dynamic pressure values obtained using the gradient boosting method. The results lie approximately along a straight line, although some scatter is evident. This deviation can be attributed to variations in the angle of attack and the sideslip angle under conditions of constant dynamic pressure.

Figure 7 shows the corresponding results obtained using the XGBoost method. Here, both the root mean square error (RMSE) and absolute error (MAE) are significantly reduced, and the data points align more closely with the one-to-one line, exhibiting less scatter than in Figure 5. Even when the angle of attack and sideslip angle vary, the XGBoost model provides more accurate dynamic pressure predictions. These findings suggest that XGBoost is the most promising method for dynamic pressure estimation among those examined thus far.

In summary, XGBoost consistently outperforms the conventional gradient boosting method for dynamic pressure prediction. Future work will extend the analysis by applying additional machine learning algorithms and conducting a broader performance evaluation.

Algorithm	RMSE (kPa)	MAE (kPa)	R <sup>2</sup>
Linear Multiple Regression	1.827	1.024	0.996
Gradient Boost	1.063	0.7156	0.999
Catboost	0.496	0.3613	1.000
Xgboost	0.0079	0.0041	1.000

**Table 1.** Evaluation and Comparison of Errors Among Algorithms

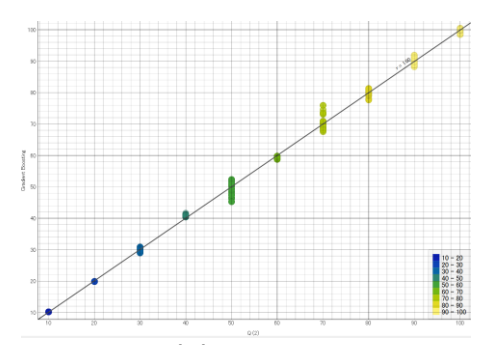


Fig 6. Plot of theoretical versus estimated dynamic pressure using the Gradient Boost method.

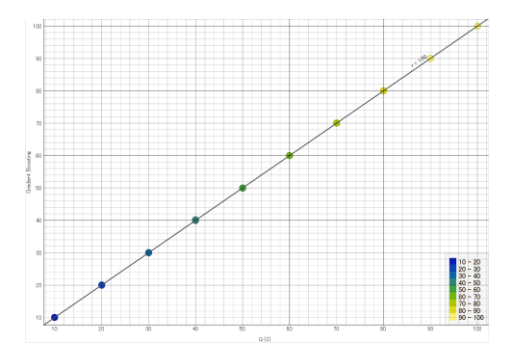
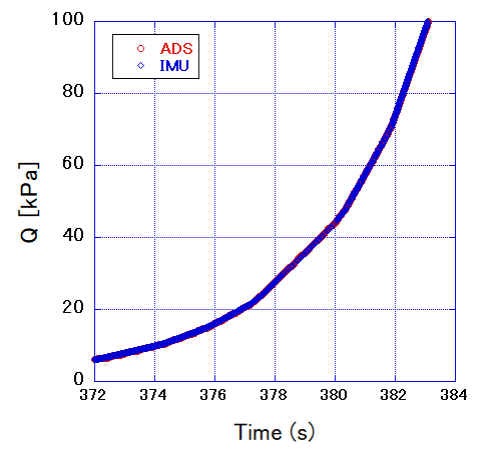


Fig 7. Plot of theoretical versus estimated dynamic pressure using the XGBoost method.

#### yhxc

A comparative analysis was carried out between flight data obtained from the onboard inertial measurement unit (IMU) and predictions generated by machine learning models. Dynamic pressure reconstructed from IMU measurements was employed as the reference for validation. As shown in Fig. 8 (372–384 s after launch), the predictions exhibit generally good agreement with the IMU-derived values, supporting the validity of the proposed estimation framework.

A closer examination reveals that discrepancies become more pronounced in the low-pressure regime, where measurement noise and the sensitivity of the models to flow conditions are relatively significant, as illustrated in Fig. 9 (372–378 s after launch). In contrast, prediction errors decrease markedly in the high-pressure regime. This behavior is consistent with the principle that high-pressure data points exert a dominant influence on the overall error metrics, as shown in Fig. 10 (378–384 s after launch). Consequently, minimizing errors in the high-pressure region contributes effectively to reducing the total error across the entire dataset.



**Fig 8.** Comparison between dynamic pressure estimated from IMU data and that predicted by machine learning during the flight test (372–384 s after launch).

HiSST-2025-40 Page | 7 Paper

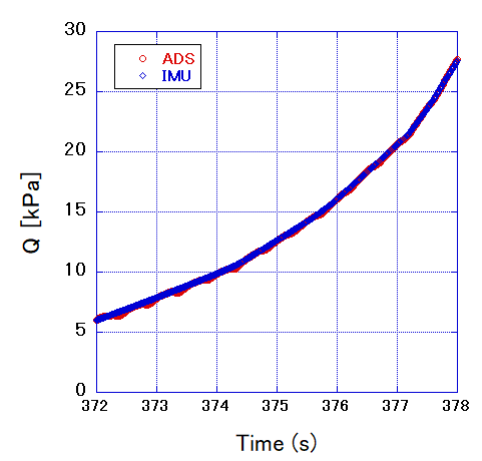


**Fig 9.** Comparison between dynamic pressure estimated from IMU data and that predicted by machine learning during the flight test (372–378 s after launch), corresponding to a low-dynamic-pressure regime.

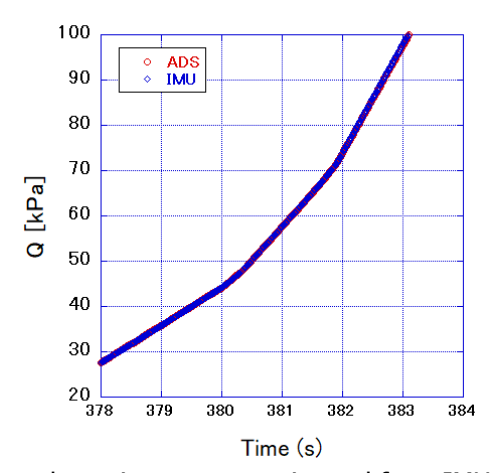


**Fig 10.** Comparison between dynamic pressure estimated from IMU data and that predicted by machine learning during the flight test (378–384 s after launch), corresponding to a high-dynamic-pressure regime.

#### Conclusion

The Japan Aerospace Exploration Agency (JAXA) conducted a hypersonic combustion flight experiment to reduce reliance on wind tunnel testing; the JAXA RD1 Flight Demonstrator was launched from the Uchinoura Space Center on July 24, 2022, and the mission was successfully completed and valuable flight data was obtained.

In this study, statistical machine learning methods were applied to estimate dynamic pressure and Mach number from the flight experiment data. Nonlinear regression techniques including gradient boosting, CatBoost, and XGBoost were introduced to extend conventional linear regression. The results demonstrated that machine learning significantly reduced the prediction error, with XGBoost having the best agreement with theoretical values.

Validation against dynamic pressure derived from IMU (Inertial Measurement Unit) further confirmed the validity of the proposed method. While some discrepancies were observed in the low-pressure region, the accuracy was significantly improved in the high-pressure region, indicating that error minimization has the greatest impact on overall prediction accuracy.

These findings support the potential that advanced machine learning, especially with XGBoost, has for accurate aerodynamic state estimation in hypersonic flight. Future work will extend this framework to a wider range of algorithms and incorporate adaptive and pressure-sensitive learning strategies to further improve robustness and generalization capabilities.

#### **Acknowledgments**

The author would like to express their sincere gratitude to Kouichiro Tani for providing the IMU and other flight test data. In addition to supplying the data, he also contributed through valuable discussions on the data analysis. The numerical calculations in this study were carried out using JAXA's JSS2 and JSS3 supercomputer systems. We also acknowledge the cooperation of many colleagues at the Institute of Space and Astronautical Science, as well as the support of rocket manufacturers and other providers.

#### References

- 1. Kanda, T., et al.: Design of sub-scale rocket-ramjet combined cycle engine model. IAC paper IAC-05-C4.5.03 (2005)
- 2. Tomioka, S., Ueda, S., Tani, K., Sakuranaka, N., Hiraiwa, T., Kanda, T.: Sea-level static tests of a rocket-ramjet combined cycle engine model. In: 43rd AIAA/ASME/SAE/ASEE Joint Propulsion Conference and Exhibit, AIAA Paper 2007-5389, Cincinnati, OH, 8–11 July 2007
- 3. Tomioka, S., Takegoshi, M., Kudo, K., Kato, K., Hasegawa, S., Kobayashi, K.: Performance of a rocket-ramjet combined-cycle engine model in ejector mode operation. In: 15th AIAA International Space Planes and Hypersonic Systems and Technologies Conference, AIAA Paper 2008-2618, Dayton, OH, Apr 2008
- 4. Tani, K., Izumikawa, M., Saito, T., Ono, F., Murakami, A.: Ram and ejector-jet mode experiments of the combined cycle engine in Mach 4 flight conditions. In: 46th AIAA Aerospace Sciences Meeting and Exhibit, AIAA Paper 2008-0103, Reno, NV, Jan 2008
- 5. Tani, K., Tomioka, S., Kato, K., Hiraiwa, T.: Current status of research of the combined cycle engine at JAXA. In: 20th ISABE Conference, ISABE Paper 2011-1334, Gothenburg, Sweden (2011)
- 6. Takegoshi, M., et al.: Mach 8 flight condition tests of rocket-ramjet combined cycle engine model. In: 49th AIAA/ASME/SAE/ASEE Joint Propulsion Conference, AIAA Paper 2013-3668, San Jose, CA, Jul 2013
- 7. Tomioka, S., Ueda, S., Tani, K., Kanda, T.: Scramjet engine tests at ramjet engine test facility in JAXA-KSPC. In: 45th AIAA Aerospace Sciences Meeting and Exhibit, AIAA Paper 2007-1040, Reno, NV, 8–11 Jan 2007
- 8. Mitani, T., Hiraiwa, T., Sato, S., Tomioka, S., Kanda, T., Tani, K.: Comparison of scramjet engine performance in Mach 6 vitiated and storage-heated air. J. Propuls. Power 13, 635–642 (1997)
- 9. Tomioka, S., Hiraiwa, T., Kobayashi, K., Izumikawa, M., Kishida, T., Yamasaki, H.: Vitiation effects on scramjet engine performance in Mach 6 flight conditions. J. Propuls. Power 23, 789–796 (2007)
- 10. Tani, K., et al.: Flight experiment for the validation of new methodology to compensate the wind tunnel contamination problem. In: 32nd ISTS, Paper 2019-g-02, Fukui, Japan (2019)
- 11. Takahashi, M., et al.: Numerical study on combustor flow-path design for a scramjet flight experiment. In: 32nd ISTS, Fukui, Japan (2019)
- 12. Kodera, M., et al.: Investigation of air vitiation effects on scramjet engine performance. In: 32nd ISTS, Fukui, Japan (2019)
- 13. Hashimoto, A., Murakami, K., Aoyama, T., Ishiko, K., Hishida, M., Sakashita, M., Lahur, P.R.: Toward the fastest unstructured CFD code 'FaSTAR'. AIAA Paper 2012-1075 (2012)
- 14. Murayama, M., Yamamoto, K., Hashimoto, A., Ishida, T., Ueno, M., Tanaka, K., Ito, Y.: Japan Aerospace Exploration Agency studies for the Fifth AIAA Drag Prediction Workshop. J. Aircraft 51, 1244–1267 (2014)
- 15. Hashimoto, A., Murayama, M., Yamamoto, K., Aoyama, T., Tanaka, K.: Turbulent flow solver validation of FaSTAR and UPACS. AIAA Paper 2014-0240 (2014)
- 16. Hasegawa, S., Kanda, T.: Preliminary numerical simulation of flow around spaceplane for airframe engine integration. In: 31st ISTS, Matsuyama, Ehime, Japan (2017). Trans. JSASS Aerospace Technology Japan

- 17. Hasegawa, S., et al.: Flow analysis around spaceplane for airframe engine integration by CFD. In: 32nd ISTS, Fukui, Japan (2019)
- 18. Obayashi, S., Guruswamy, G.P.: Convergence acceleration of an aeroelastic Navier–Stokes solver. AIAA J. 33, 1134–1141 (1995)
- 19. Men'shov, I., Nakamura, Y.: Implementation of the LU-SGS method for an arbitrary finite volume discretization. In: 9th Japanese Symposium on CFD, Tokyo, Japan, pp. 123–124 (1995)
- 20. Shima, E., Kitamura, K., Haga, T.: Green–Gauss/weighted-least-squares hybrid gradient reconstruction for arbitrary polyhedra unstructured grids. AIAA J. 51, 2740–2747 (2013)
- 21. Hishida, M., Hashimoto, A., Murakami, K., Aoyama, T.: A new slope limiter for fast unstructured CFD solver FaSTAR. JAXA-SP-10-012, pp. 85–90 (2011) (in Japanese)
- 22. Turbulence Modeling Resource: <a href="http://turbmodels.larc.nasa.gov/">http://turbmodels.larc.nasa.gov/</a> (accessed 4 Aug 2025)
- 23. Hasegawa, S., Tani, K.: Numerical study of JAXA's experimental vehicle for hypersonic flight. In: 71st International Astronautical Congress (IAC) The Cyber Space Edition, Paper IAC-20-C4.7.5, Paris, Oct 2020
- 24. Takahashi, H., et al.: Flush air-data sensing system for a sharp-nosed hypersonic vehicle with curved-wedge forebody. AIAA J. 58(11), Oct 2020
- 25. Tani, K., Takegoshi, M., Takasaki, K., Tokudome, S.: JAXA RD1 flight experiment on supersonic combustion: Part 1. Overview. In: 25th AIAA International Space Planes and Hypersonic Systems and Technologies Conference, Bengaluru, India, 28 May–1 Jun 2023
- 26. Bishop, C.M.: Pattern Recognition and Machine Learning. Springer, New York (2006)
- 27. Chen, T., et al.: XGBoost: A scalable tree boosting system. arXiv preprint arXiv:1603.02754 (2014). https://arxiv.org/abs/1603.02754
- 28. Prokhorenkova, L., et al.: CatBoost: Unbiased boosting with categorical features. arXiv preprint arXiv:1706.09516 (2017). https://arxiv.org/abs/1706.09516